

Testing different strategies for the Remediation of Soils Polluted with Lindane

J. Vidal¹, M. Carvela², C. Saez^{2,*}, P. Cañizares², V. Navarro³, R. Salazar¹, M.A. Rodrigo²

¹ Departamento de Química de los Materiales. Facultad de Química y Biología. Universidad de Santiago de Chile. Chile

² Departamento de Ingeniería Química. Facultad de Ciencias y Tecnologías Químicas. Universidad de Castilla La Mancha. Campus Universitario s/n. 13071 Ciudad Real. Spain.

³Geoenvironmental Group, Civil Engineering School, University of Castilla-La Mancha, Avda. Camilo José Cela s/n, 13071 Ciudad Real, Spain

Abstract

Keywords

Soil remediation, electrokinetic soil flushing, permeable reactive barriers, clopyralid

*Author to whom all correspondence should be addressed: cristina.saez@uclm.es

1. Introduction

At the end of the 1950s, organochlorinated products began to be produced on a large scale throughout the World. One of the most commercialized was lindane (γ -hexachlorocyclohexane, HCH) widely used for agricultural activities, forestry and even for domestic applications ([Abhilash et al., 2013](#)).

Lindane is a persistent substance found in polluted soils and waters and susceptible to be bioaccumulated and biomagnified in the trophic chain. Numerous effects in animals and humans (neurologic, hepatic, immunologic and reproductive system) have been described ([Santos et al., 2018](#)). Likewise, the IACR (International Agency for Cancer Research) classifies the lindane as carcinogenic to humans within Group 1, where the most dangerous contaminants can be found. Similarly, due to its toxicity, liposolubility (bioaccumulation), volatility (transport) and persistence in the environment, it has been included in the list of persistent organic pollutants of the Stockholm Convention ([Muñoz-Morales et al., 2017](#)). Because of that, currently, lindane is banned in many countries, including Spain, which halted its use massively by the early 90s. However, to this day, there are well-known contamination points that cause great social concern ([Fernández et al., 2013](#)) and which are becoming a very serious environmental problem. Fortunately, Society has become aware of the need to prevent and remediate soil contamination. This is reflected in stricter regulations in developed countries which lead to a quest for new technologies capable to remove this kind of pollution.

One very promising remediation technology is the electrokinetic remediation of soils, which is based on the application of an electric field between two or more electrodes inserted in the soil capable to induce transport phenomena such as electromigration, electroosmosis and electrophoresis, which are responsible for the mobilization of species

(ions, water and charged compounds, respectively) contained in contaminated soils (Rodrigo et al., 2014). As result of these electrochemically-induced processes, changes are also observed in the pH of the soil in the vicinity of the electrodes by the action of water electrolysis. As well, an increase in temperature can also be observed, caused by the ohmic resistance of the soil. All of these processes interact with each other and with other physical and chemical processes such as: ion exchange, precipitation, volatilization, etc., which produce changes that, when properly designed, contribute to the elimination of soil contaminants (Reddy & Cameselle 2009).

In the literature, several works can be found that address these processes (Ribeiro et al., 2005, Ribeiro et al., 2011, Lima et al., 2012, López-Vizcaíno et al., 2014, Mena et al., 2015; Dos Santos et al., 2016; Risco et al., 2016b). Most of them are performed on a laboratory scale, because it is the size which allows the easier characterization and fitting of the parameters of the system, providing a good description of the mathematical model of the process. However, conclusions drawn at lab or bench-scale cannot easily be extrapolated to the full scale. Thus, in our research group, different processes for the electrochemical remediation of soils have been evaluated at different scales pointing out the relevance of this input (Risco et al., 2016a, Souza et al., 2016, López-Vizcaíno et al., 2017a, López-Vizcaíno et al., 2017b; Rodrigo et al., 2018). Recently, in our research group, we evaluated the use of permeable reactive barriers (PRB) between the electrodes, which have been used as an in-situ technology for the remediation of contaminated sites (Araujo et al., 2016). In general, a PRB is constructed perpendicular to the groundwater flow and below the phreatic level so that the natural hydraulic gradient carries the contaminant through the reactive medium of the PRB and can degrade or immobilize it as water flows through the barrier. Previous works focused on the use of Granular Activated Carbon and

biological barriers for the remediation of soils polluted with different species also pointed out the relevance of this technology for the removal of this species (Ruiz et al., 2013; Souza et al., 2017; Sun et al., 2017). Also, in a recent study (Vidal et al., 2018), it was evaluated the use of, two types of zero valent iron (ZVI) PRBs (nano-ZVI and milli-ZVI) that were used as a quick treatment that managed to reduce the hazardousness of the halogenated pollutant contained in the soil; thus, transforming it in a less dangerous non-halogenated species. In that case the pollutant was clopyralid, which is known to be highly soluble in water and do not require for the addition of surfactants to improve its mobilities under the application of electric fields.

With this background, the objective of this work has been to evaluate the coupling of electro-kinetic soil flushing (*EKSF*) with three permeable reactive barriers (PRB) composed with nanoparticles of ZVI (n-ZVI), granular particles of ZVI (m-ZVI) or granular activated carbon (GAC), respectively, in order to remediate soil polluted with lindane. Lindane is known to have less mobility than clopyralid but with the use of the surfactant SDS, its transport is expected to be enhanced. Thus, it is expected that ZVI-barriers will contribute to the transformation of the halogenated pollutant into less-hazardous non-halogenated species, whereas the activated carbon will contribute to retain the organics mobilized through the soil by *EKSF* process. Nevertheless, their behavior as PRB is not well described in literature and further research is required. In this work, six different test are schedule: i) a reference test to determine the contribution of non-EK processes, ii) a conventional *EKSF* and a daily reverse polarity *EKSF* to determine the mobility of lindane in soil, iii) *EKSF* combined with two types of ZVI barriers (nZVI-PRB and mZVI-PRB) and iv) *EKSF* modified with a PRB of activated carbon (GAC-PRB).

Results will be compared in terms of mobilized fluid, changes induced in pH and conductivity and the final distribution of the pollutant and its reaction products.

2. Materials and methods

Materials. In this study, in order to reproduce actual conditions and increase the reliability of the results obtained, we used a natural soil of a quarry located in Mora (Toledo, Spain), whose mineralogical composition was determined by X-ray diffraction analysis: Quartz 7%, Feldspar 15%, Calcite 4%, Kaolinite 26%, Smectite 28%, Illite 20% and Organic content 0%. Lindane (CAS number: 58-89-9, C₆H₆Cl₆, 97% of purity) was selected as model of commercial herbicide and it was used as received. Sodium Dodecyl Sulfate (SDS) (used as solubilizing agent) and Hexane (Sigma Aldrich, Spain) were analytical grade and used as received. Ethyl Acetate high pure were obtained from Sigma Aldrich and used for GC-ECD. Two types of iron were tested: micro iron ($\geq 99\%$), reduced, powder (fine) purchased from Sigma Aldrich and Nanofer Star (NanoIron, Czech Republic), which is a dry air-stable nZVI powder used as received. Granular Active Carbon (Chemviron, Feluy, Belgium) was used as received.

Experimental design. The experimental installation consists of methacrylate reactors with a capacity of 175 dm³. The volume of total soil used is 139.6 dm³, composed of four layers (course gravel, sand, clay and sand capillary barrier) as described elsewhere ([Lopez-Vizcaino et al., 2011](#)). To obtain a homogeneous compaction similar to a clay soil in its natural state a proctor compaction test was carried out ([Lopez-Vizcaino et al., 2011](#)).

Six different tests were carried out: 1) reference test to check the natural dispersion of lindane (*no-EK*), 2) electrokinetic soil-flushing test with facing rows of electrodes (*EKSF*),

3) reversible electrokinetic soil-flushing test in which polarity of electrodes was daily changed (*REKSF*), 4) electrokinetic adsorption barrier (*EKAB*), 5) electrokinetic nano-ZVI barrier (*EKnZVIB*), 6) electrokinetic mili-ZVI barrier (*EKmZVIB*). Except for the reference test *no-EK*, the electrodes were positioned in semipermeable electrolyte wells, in order to facilitate the extraction of the effluents generated in the process. The configuration of electrodes used consists of two rows of three wells facing each other and separated by 38 cm ([Figure SM1](#)). In the third system, an activated carbon barrier ($1 \times 38 \times 16$ cm) was positioned at an equidistant distance from electrode rows. It consists of a mixture of 120 g of activated carbon and 450 g of soil. In the four and fifth tests, a permeable reactive barrier of zero-valent iron particles with dimensions of $1 \times 38 \times 16$ cm (width, length and depth) was positioned at a distance of 2 cm from the anodic wells with an amount of 203.04 g or 266.79 g of nano or fine-grained zero-valent iron particles, respectively. The electrode materials used are graphite rods with dimensions $1 \times 1 \times 10$ cm³. The electrolyte wells have coupled a level control system connected to the feed tank to regulate the added volume of water to the soil. In cathode wells, level controls connected to peristaltic pumps have been introduced to extract the volume of surplus water. After the installation of the wells, tensiometers are inserted, which allow to analyze the amount of water that the soil has in continuous, and thermocouples to monitor the temperature. In addition, to collect the contaminant from the evaporation flows, in each mockup a cylindrical adsorption column of 1 cm in diameter and 20 cm in length filled with activated carbon were connected. Once the assembly is complete, the soil is contaminated drop by drop (simulating an accidental leakage) with an equivalent dose of 10 mg of Lindane / kg of soil, leaving 24 h for the dispersion of the contaminant through the reactor after the complete dose of pollutant.

To begin operating, the electrolyte wells were completely filled with water. The electric current was supplied by a power supply SM 400-A R-8 DELTA ELEKTRONIKA BV in potentiostatic work mode applying 1 V cm^{-1} . The electrokinetic experimentation lasted approximately 720 hours. Over this time, it was controlled the amount of electrolyte supplied in anodes and that collected in cathodes, the drain valve, the intensity of current, the pH, the conductivity and concentration of lindane and intermediates in electrolyte wells. At the end of the experiments, the soil underwent a postmortem analysis, being divided in order to obtain surface and depth maps of pH, conductivity, moisture, lindane concentration and intermediates (Risco et al., 2016a; Risco et al., 2016b).

Apparatus and analytical procedures. To determine lindane concentration in the liquid phase, an L–L extraction process was used before the analysis. This process was carried out in separator flasks of 10 mL, using ethyl acetate as extraction solvent (ratio lindane solution/solvent = 1 v/v is required to extract 100% of lindane contained in the aqueous phase). After that, all samples extracted from electrolyzed solution were filtered with $0.25 \mu\text{m}$ nylon filters before analysis by Gas Chromatography-Electron Capture Detector (GC ECD) (Thermo Fisher Scientific) using a TG-5MS capillary column ($30 \text{ m} \times 0.25 \text{ mm}$ 0.25 mm) and ^{63}Ni micro-electron capture detector, a split/splitless injector and ChromCard Software. Under the conditions used, the quantification limit of the GC ECD was 0.02 mg L^{-1} . The flow rate of gas He was 1.0 mL min^{-1} . The temperature of the injector was $210 \text{ }^\circ\text{C}$. The pH and conductivity were measured with the help of a Crison GLP 22 pH meter and a Crison Ecmeter Basic 30+ conductivity meter. During the postmortem analysis, soil samples were taken and the pH and conductivity were measured with the same S-L extraction procedure previously described. The humidity was measured

using different procedures depending on whether the measurements were carried out continuously or discontinuously. The discontinuous measurements were made by thermogravimetry, whereas the continuous measurements were made indirectly by analyzing the suction that the soil presents (Risco et al., 2015). The suction values are determined by a set of tensiometers model T5 (UMS GmbH, Munich, Germany) inserted directly on the ground, and connected to a datalogger model DL6 (UMS GmbH, Munich, Germany) that automatically stores data with an interval of 20 minute sampling. The temperature of the soils was obtained through the insertion of ECT model thermocouples (Decagon Devices, Pullman, USA). The data collection was carried out by connecting these sensors to an Em5B data logger (Decagon Devices, Pullman, USA) that has 5 acquisition channels and automatically stores data with a sampling interval of 20 minutes. The colorimetric method used to determine the concentration of the SDS surfactant has been described elsewhere (Jurado et al., 2006).

3. Results and discussion

Before starting with the remediation procedures, an accidental spill was induced in the six mockups, in order to simulate a real case of pollution with a non-homogeneous distribution of pollutants. Then, after dosing the pollutants, the mockups were not handled for 24 h, in order to promote the natural dispersion of the pollutant throughout the mockups. After that, the operation started with the application of 1.0 V cm^{-1} of electric field between the rows of anodes and cathodes inserted in electrolyte wells. This electric field was maintained for 720h, except for the case of the reference test (*no-EK* test) which was not operated during this period. This test was carried out to help to elucidate the removal related to non-

controlled mechanisms. In all tests, during operation, many variables were monitored, including operation parameters and soil and electrolyte parameters.

Figure 1-a shows the changes in the electric current intensity during the *EK-PRB* tests with the three types of barrier tested in this work: *EKnZVIB*, *EKmZVIB* and *EKAB*. As it can be observed, despite: (1) all mockups were operated in potentiostatic mode under the same electric field and (2) the mockups were prepared with the same procedure and electrodes were placed in the same position, there are significant differences among the intensities reached and their time-changes during the tests. This means that the insertion of a PRB has a significant influence on the reaction and transport rates underwent by species contained in soil. Thus, as seen, the intensity reached seems to depend on the size and materials of the reactive particles contained in the PRB. It decreases in the sequence *EKAB-EKMZVIB-EKnZVIB* (as summarized in Figure 1b), which is the same sequence of the sizes of the particles contained in the reactive barrier. This observation can be explained because for the same mass ratio, the larger particles affect in lower extension to the continuity of soil contained in the PRB, decreasing more importantly the ohmic losses that it may cause. That is, the soil is more homogeneous when using larger particles than when using lower size particles because the PRB can be more easily and uniformly compacted. In addition, another explanation can also help to support the observations: particles of GAC and iron are electrically-conductive. This means that inside the electric field generated between the two rows of electrodes they behave as bipolar electrodes. In this case, the lower size produces a higher bipolar electrode surface area which disturbs more the current distribution lines. In addition, iron is more conductive than GAC, also helping to explain the experimental differences observed. Fluctuations in the values of intensity account for the high

complexity of this multiparametric system, for which despite of the strictly controlled conditions, there are many inputs affecting the system at a time.

Anyway, these values are quite similar to the values registered in previous electro-remediation tests in which *EKSF* and *EKAB* and reversible EK adsorption barrier (*REKAB*) technologies were evaluated for the remediation of soils polluted with other pesticides and organochlorinated organics (Rodrigo et al., 2014a; Risco et al., 2015; Risco et al., 2016a; Risco et al., 2016c; Risco et al., 2016d; Risco et al., 2016e; Risco et al., 2016f) and this fact indicates the robustness of the methodology developed in these tests. Another important observation which can be drawn from Figure 1b is that the use of reversible polarity (without barriers) also affects negatively the current flow. As reported in previous studies (Rodrigo et al., 2018), these differences can also be related to changes in the conductivity and pH of the soil during the treatment. The reversion in the polarity of the electrodes' rows neutralize the acidic and basic fronts contributing to a decrease in the conductivity. Meanwhile, other anions and cations are attracted towards the electrode rows, decreasing the ionic conductivity in the central position and contributing to a lower exerted intensity.

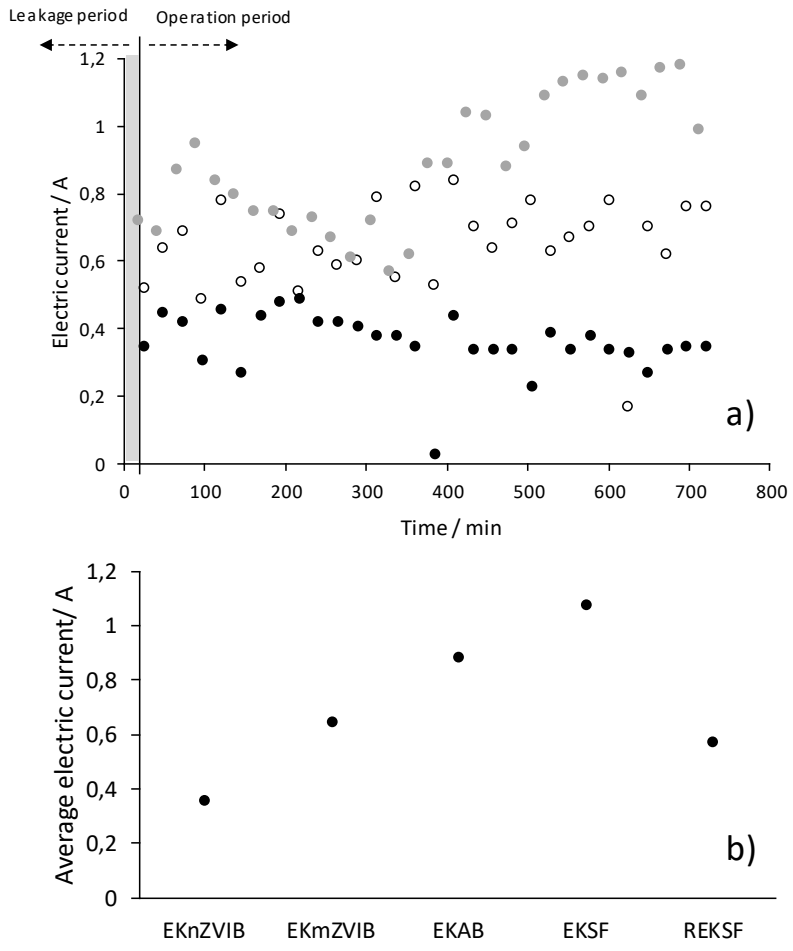


Figure 1. a) Time-course of the changes observed in the intensity exerted in the three PRB-EKSF: ● *EKnZVIB*; ○ *EKmZVIB*, ● *EKAB*. b) Average electric current in the five EK-strategies tested. Electric field of 1.0V cm^{-1} .

Figures 2 and 3 shows the 2-D distribution maps of pH and conductivity in the six mockups. As can be observed in Figure 2, the final pH-profiles are quite different. In *no-EK* test, as expected, pH values are homogeneous and close to neutrality. Similar profile was obtained

Comentado [MARR1]: Hacer mapas 2-D con la media de las tres alturas e incluir los 6 paneles (uno por test) para conductividad y para pH

in REKSF, as in previous works where reversible polarity strategies were tested (Ref Sandra chemosphere). On the other hand, a market profile is observed in the case of using adsorption barrier: very alkaline pH in the soil sited between cathodic wells and the PRB, and slightly acid in the anodic side. On contrary, when ZVI is used as PRB the alkaline front does not seem to be as relevant, while in acid front is observed close to anodic wells. This is even more relevant when granular particles are used. Regarding final soil conductivity (Figure 3), differences are less significant, although again, *REKAB* conductivity profile seems to be more noteworthy than the other one.

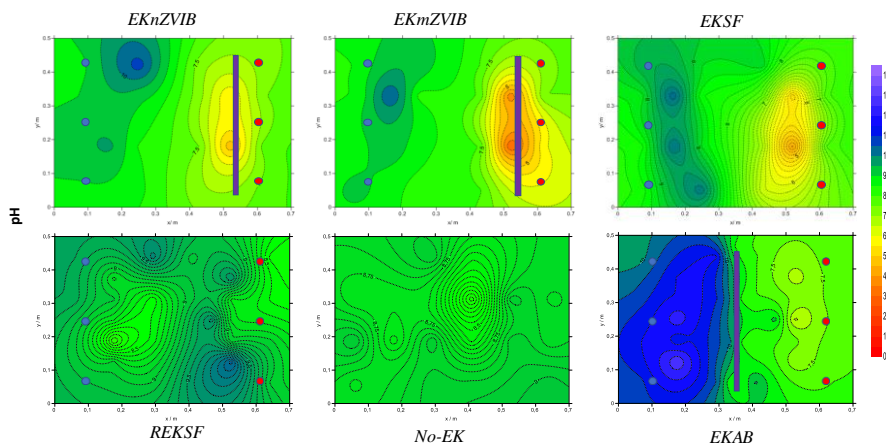


Figure 2. 2-D plots of the final pH of the soil after electroremediation tests.

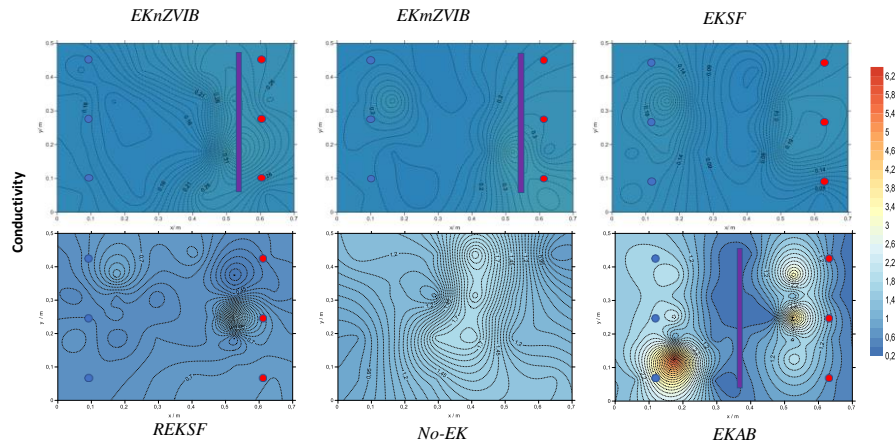


Figure 3. 2-D plots of the final conductivity of the soil after electroremediation tests.

Figure 4 shows the average temperature registered in the soil during the five electroremediation tests. As expected, because of the higher intensity reached (ohmic losses depends on the square of the intensity), the average temperature was higher during EKSF test (29.2 °C), while it ranges around 26°C or 24°C in the other cases. Anyhow, differences between averaged temperatures are not very important, in particular if it is taken into account the high number of inputs that can influence on it (not only the ohmic resistance but also the evaporative cooling and other factors).

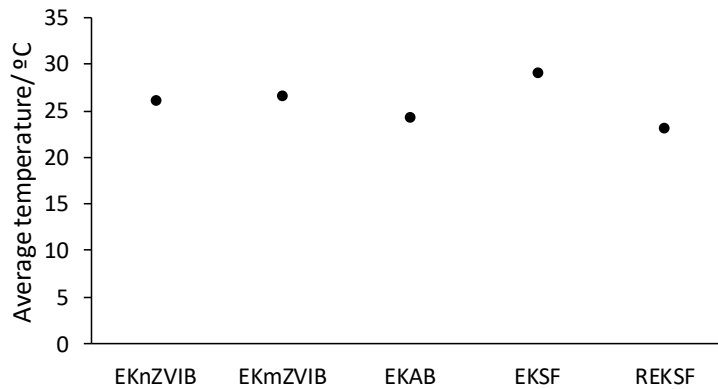


Figure 4. Average temperature of the soil during electroremediation tests. Electric field of 1.0V cm^{-1} .

To evaluate the influence of the electroremediation strategy used in water and pollutant fluxes, both volume of electrolyte mobilized and lindane extracted in each case are plotted respect to that obtained in the EKSF test (selected as EK-reference test for this comparison). Thus, Figure 5 shows the increase (or decrease) of the water amount (used as flushing fluid) added in anodic wells, or extracted in cathodic wells and by gravity flux in *EKnZVIB*, *EKmZVIB*, *EKAB* and *REKSF* respect to *EKSF* test (56.3 L added, 17.1 L extracted from cathodes and 7.9 L extracted by gravity flux), while Figure 6 shows this comparison in terms of lindane extracted (*EKSF* test: 1.08 mg extracted from anodes, 2.21 mg extracted from cathodes and 4.4 mg extracted by gravity flux).

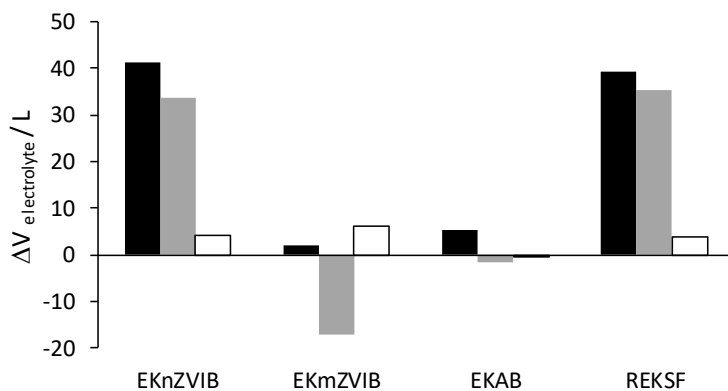


Figure 5. Changes (positive or negative) of volume of electrolyte added in anodic wells, or extracted in cathodic wells and by gravity in *EKnZVIB*, *EKmZVIB*, *EKAB* and *REKSF* respect to *EKSF* test (56.3 L added, 17.1 L extracted from cathodes and 7.9 L extracted by gravity flux). Electric field of 1.0V cm^{-1} . ■ Electrolyte added to anodic wells, ■ Electrolyte extracted from cathodic wells and □ electrolyte-gravity flow.

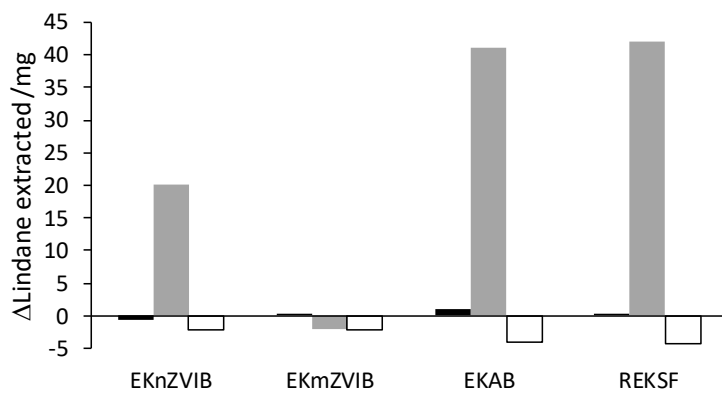


Figure 6. Changes (positive or negative) in the amount of lindane extracted in *EKnZVIB*, *EKmZVIB*, *EKAB* and *REKSF* respect to *EKSF* test (1.08 mg extracted from anodes, 2.21 mg extracted from cathodes and 4.4 mg extracted by gravity flux). Electric field of 1.0V cm^{-1} . ■ Anodic wells, ■ Cathodic wells and □ gravity flow.

As can be observed, in terms of water mobility there are great differences between *EKSF* and *REKSF* and *EKnZVIB* tests. On contrary, in the case of *EKmZVIB* and *EKAB* the volume of water added to maintain the electrolyte level in the anodic wells (58.3 and 61.6 L, respectively) was only slightly higher than that required in *EKSF* test (56.3 L). The daily change of polarity in *REKSF* test seems to favour the movement of water through the soil in comparison with other strategies tested. Likewise, the use of nZVI in the reactive barriers also seems to induce the transport of water. This could be related to the changes induced in the current lines by nZVI particles used in the reactive barrier, that can behave as bipolar electrodes and, thus, modify the behaviour of the system. However, this is not observed in the case of granular particles (mZVI), which seem to act as EK-barrier to the passage of water (the volume of water extracted from cathodic wells was nil in this case). In the case of *EKAB* the electroosmotic flux is quite similar to that of *EKSF*, while it is significantly higher in *REKSF* and *EKnZVIB* tests. This agrees with the higher demand of water observed in anodic wells. Respect to gravity flux, the differences are less relevant.

Figure 7 shows the 2-D distribution maps of water content in the soil after the treatment. As seen,

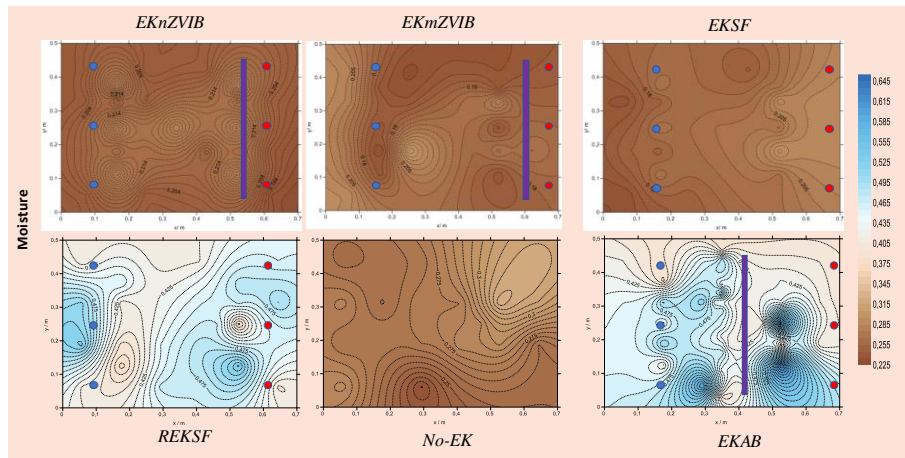


Figure 7. 2-D plots of the final moisture of the soil after electroremediation tests.

In terms of lindane mobilization, the differences are even more remarkable. However, it is important to point out that this Figure only summarizes the amount of lindane extracted with the aqueous phase, but it is well-known that in presence of iron particles (naturally contained in soil or added in the ZVI barrier) lindane can suffer a rapid dehalogenation, and that activated carbon shows a very good adsorption capacity for lindane in aqueous phase (REF martin). Therefore, both processes must be taken into consideration to explain the overall remediation, as it will be discussed later on. Anyway, in Figure 6 it can be observed that the amount of lindane extracted from anodic side in all strategies is quite similar: 0.41, 1.37, 2.18 and 1.48 mg in *EKnZVIB*, *EKmZVIB*, *EKAB* and *REKSF*, respectively, versus 1.08 mg of lindane extracted in *EKSF* test. Similar amounts are also dragged by gravity flux: 2.13, 2.23, 0.32 and 0.05 mg in *EKnZVIB*, *EKmZVIB*, *EKAB* and *REKSF*, respectively, versus 4.4 mg dragged in *EKSF* test. On contrary, great differences are

observed in the amount of lindane dragged with electroosmotic flux to cathodic wells, where *EKnZVIB*, *EKAB* and *REKSF* are able to mobilize 22.31, 43.45 and 44.19 mg of lindane, respect to 2.21 mg fluxed during *EKSF* test. These results agree with the higher electroosmotic flux detected in *EKnZVIB* and *REKSF* tests, although the low water flux observed in *EKAB* is not able to explain the high amount of lindane dragged. These differences are not observed in terms of SDS (data not shown): SDS extracted ranges within the range 25 - 45 mg, which is not relevant taking into account the total amount added initially (around 10000 mg of SDS) during the simulated spill of lindane SDS-aqueous solution. This means that almost all the surfactant added with lindane during the leakage remains in the soil after EK process.

Nevertheless, in spite of the differences observed among EK-tests, the amount of lindane mobilized by flushing fluid is very low. Thus, to verify their retention in the soil a deep analysis of the soil and activated carbon was done after 720 h of operation (post-mortem characterization of the soil). For comparison purpose, a test in which soil does not undergo electrokinetic treatment was also done in order to quantify the losses of lindane related to the contribution of non-electrokinetic transport mechanisms such as volatilization or to its chemical reactivity in the soil. In fact, it is reported that iron naturally contained in soil (around 3% of FeO_3) can favour dehalogenation mechanism (ref). Figure 8 shows the 2-D plot of lindane remaining in the soil after the electrokinetic processes and the reference tests (without applying electric field).

Comentado [MARR2]: De momento ok

Comentado [MARR3R2]: Hace falta mapa 2d de humedad en las maquetas al final del tratamiento

Comentado [CSJ4R2]: He incluido la figura, pero no acabo de ver que ayude mucho. EKAB y REKSF acumulan más agua pero no acabo de ver relación con la gráfica anterior

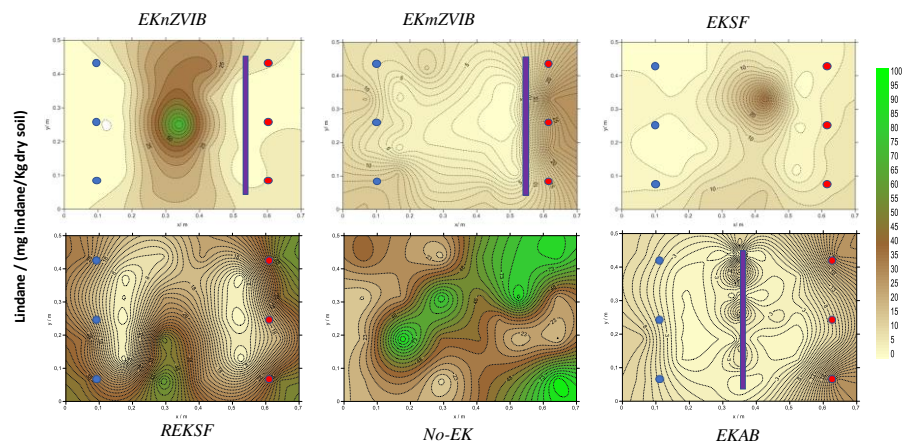


Figure 8. 2-D plots of lindane (mg) in the soil after electroremediation tests.

As can be observed, after 720 h from the spillage, the distribution of lindane in the soil that does not undergo EK-process is not homogeneous. In total, around 94 % of the lindane dispersed initially remains in the soil, and, thus, only 6 % is lost or transformed. In this test, apart from lindane no organics were detected in the soil during the post-mortem test, indicating that at this condition natural dehalogenation does not take place and that volatilization seems to be the main side process. However, it was not retained (or at least, it was not quantified) in the adsorption column placed in the system to capture volatile organics.

On contrast, the amount of lindane that remains unaltered in the soil after the EK processes is significantly lower: 24.5, 67.3, 48.1, 33.7, 20.3 % in *EKSF*, *REKSF*, *EKnZVIB*, *EKmZVIB*, *EKAB*, respectively. In the case of placing activated carbon barrier the retention of lindane is expected (REF martin). In fact, during post-mortem analysis, 183 mg of lindane (8,87 % of the initial lindane) were quantified in the activated carbon barrier,

whereas only 3 mg were retained (and quantified) in the adsorption column through gas phase passes. Likewise, after electroremediation tests other organics were detected both in soil and PRB. Figure 9 shows the 2-D of intermediates detected in the soil and barrier after EK-tests. As can be observed, four organics were detected in the soil, being mainly accumulated in the activated carbon barrier. Two of them, which were also detected in the other EK-tests, were identified as 3,4,5,6-tetracloro-1-ciclohexeno and 2-propanona-1,1,3,3-tetracloro. This indicates that activated carbon barrier has a great impact on results but also iron contained in the soil seems to promote the transformation of the raw lindane in dehalogenated intermediates. Therefore, it may be assumed that the electric field applied activates the removal of lindane from soil by different processes and, thus, the clarification of the remediation mechanisms involved is required to determine the most appropriate strategy.

Comentado [CSJ5]: Te paso las figuras en el power point para que veas lo que sale y ya decidimos figura, por no marear mucho a Mireya y Jorge

Figure 5. 2-D plots of lindane and intermediates (in units of chromatographic area) in the upper zone of the soil after EKAB. **NO TENEMOS TODOS LOS MAPAS DE INTERMEDIOS. En algunas maquetas no se ven. ESTOY PENDIENTE DE QUE ME PASEN MAPAS DE LAS MAQUETAS CON ZVI**

Comentado [MARR6]: Idem a figura anterior con los intermedios (en apéndice). Aquí total de intermedios en suma de areas

Figure 6 summarizes the final distribution of lindane in the electrokinetic processes tested, as well as that of the mockup non operated (no-EK). As can be observed, in all cases the percentage of lindane extracted is very low (below 2 %) while the percentage retained in soil after 720 h of treatment depends on the strategy used. In fact, the use of REKSF seems to prevent lindane removal (67 %) while EKSF and EKAB lead to the higher removal.

Relevant differences are also observed between the two mockups with ZVI barriers. The use of nanoparticles of ZVI seems to behave worst than granular ZVI (m-ZVI) in terms of lindane removal, which may be related to the dehalogenation reaction rate. According to equation 1 (where in R indicates the hydrocarbon group and X the halogen atoms) chloride and ferrous ions are released to the wastewater, while acidity is consumed and thus, changes in the pH can be observed.

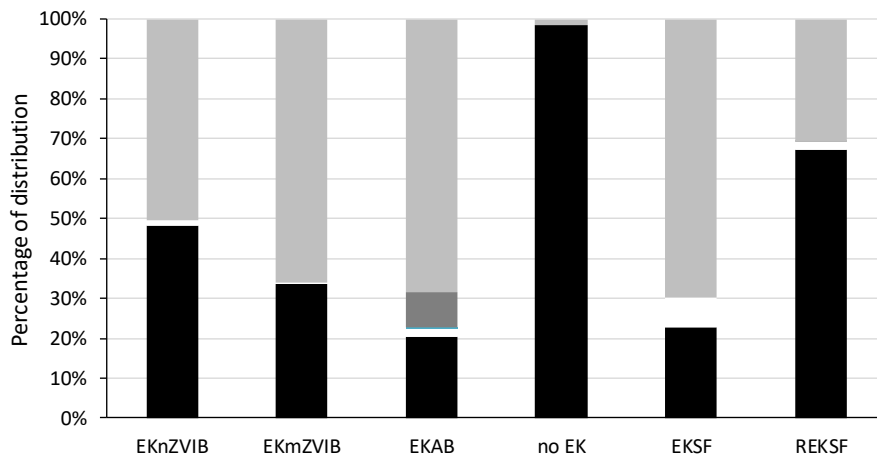
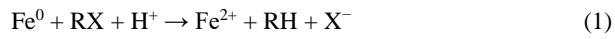


Figure 6. Final distribution of lindane after 720 h of treatment. ■ Remained in soil, □ extracted with flushing fluid, ■ adsorbed in PRB (INCLUDING INTERMEDIOS RETENIDOS??), ■ Volatilized or transformed.

Conclusions

From this work, the following conclusions can be drawn:

–

Acknowledgements

Financial support from the Spanish Ministry of Economy, Industry and Competitiveness, European Union through project CTM2016-76197-R (AEI/FEDER, UE) is gratefully acknowledged. J. Vidal thanks CONICYT for the National PhD scholarship 21140248 and DICYT USACH

References

1. Abhilash, P. C., Singh, B., Srivastava, P., Schaeffer, A., & Singh, N. (2013). Remediation of lindane by *Jatropha curcas* L: utilization of multipurpose species for rhizoremediation. *Biomass and bioenergy*, 51, 189-193.

2. Araujo, R., Castro, A. C. M., Baptista, J. S., & Fiuza, A. (2016). Nanosized iron based permeable reactive barriers for nitrate removal—Systematic review. *Physics and Chemistry of the Earth, Parts A/B/C*, 94, 29-34.
3. dos Santos, E. V., Souza, F., Saez, C., Cañizares, P., Lanza, M. R. V., Martinez-Huitle, C. A., & Rodrigo, M. A. (2016). Application of electrokinetic soil flushing to four herbicides: a comparison. *Chemosphere*, 153, 205-211.
4. Fernández, J., Arjol, M. A., & Cacho, C. (2013). POP-contaminated sites from HCH production in Sabiñánigo, Spain. *Environmental Science and Pollution Research*, 20(4), 1937-1950.
5. Lima, A. T., Kleingeld, P. J., Heister, K., & Loch, J. G. (2012). In situ electro-osmotic cleanup of tar contaminated soil—Removal of polycyclic aromatic hydrocarbons. *Electrochimica Acta*, 86, 142-147.
6. López-Vizcaíno, R., Alonso, J., Canizares, P., Leon, M. J., Navarro, V., Rodrigo, M. A., & Sáez, C. (2014). Removal of phenanthrene from synthetic kaolin soils by electrokinetic soil flushing. *Separation and Purification Technology*, 132, 33-40.
7. López-Vizcaíno, R., Risco, C., Isidro, J., Rodrigo, S., Saez, C., Cañizares, P., & Rodrigo, M. A. (2017). Scale-up of the electrokinetic fence technology for the removal of pesticides. Part I: Some notes about the transport of inorganic species. *Chemosphere*, 166, 540-548.
8. López-Vizcaíno, R., Risco, C., Isidro, J., Rodrigo, S., Saez, C., Cañizares, P., & Rodrigo, M. A. (2017). Scale-up of the electrokinetic fence technology for the removal of pesticides. Part II: Does size matter for removal of herbicides?. *Chemosphere*, 166, 549-555.

9. Lopez-Vizcaino, R., Saez, C., Mena, E., Villasenor, J., Canizares, P., Rodrigo, M.A., (2011). Electro-osmotic fluxes in multi-well electro-remediation processes. *Journal of Environmental Science and Health Part a-Toxic/hazardous Substances & Environmental Engineering* 46, 1549-1557.
10. Mena, E., Ruiz, C., Villaseñor, J., Rodrigo, M. A., & Cañizares, P. (2015). Biological permeable reactive barriers coupled with electrokinetic soil flushing for the treatment of diesel-polluted clay soil. *Journal of hazardous materials*, 283, 131-139.
11. Muñoz-Morales, M., Braojos, M., Sáez, C., Cañizares, P., & Rodrigo, M. A. (2017). Remediation of soils polluted with lindane using surfactant-aided soil washing and electrochemical oxidation. *Journal of hazardous materials*, 339, 232-238.
12. Reddy, K. R., & Cameselle, C. (2009). Overview of electrochemical remediation technologies. *Electrochemical Remediation Technologies for Polluted Soils, Sediments and Groundwater*, 1-28.
13. Ribeiro, A. B., Mateus, E. P., & Rodríguez-Maroto, J. M. (2011). Removal of organic contaminants from soils by an electrokinetic process: the case of molinate and bentazone. *Experimental and modeling. Separation and Purification Technology*, 79(2), 193-203.
14. Ribeiro, A. B., Rodríguez-Maroto, J. M., Mateus, E. P., & Gomes, H. (2005). Removal of organic contaminants from soils by an electrokinetic process: the case of atrazine.: *Experimental and modeling. Chemosphere*, 59(9), 1229-1239.
15. Risco, C., López-Vizcaíno, R., Sáez, C., Yustres, A., Cañizares, P., Navarro, V., & Rodrigo, M. A. (2016a). Remediation of soils polluted with 2, 4-D by electrokinetic soil flushing with facing rows of electrodes: a case study in a pilot plant. *Chemical Engineering Journal*, 285, 128-136.

16. Risco, C., Rodrigo, S., Lopez-Vizcaino, R., Yustres, A., Saez, C., Canizares, P., Navarro, V., Rodrigo, M.A., (2015). Electrochemically assisted fences for the electroremediation of soils polluted with 2,4-D: A case study in a pilot plant. *Separation and Purification Technology* 156, 234-241.
17. Risco, C., Rodrigo, S., Vizcaíno, R. L., Yustres, A., Saez, C., Cañizares, P., & Rodrigo, M. A. (2016b). Removal of oxyfluorfen from spiked soils using electrokinetic soil flushing with linear rows of electrodes. *Chemical Engineering Journal*, 294, 65-72.
18. Rodrigo, M. A., Oturan, N., & Oturan, M. A. (2014). Electrochemically assisted remediation of pesticides in soils and water: a review. *Chemical reviews*, 114(17), 8720-8745.
19. Rodrigo, S., Saez, C., Cañizares, P., & Rodrigo, M. A. (2018). Reversible electrokinetic adsorption barriers for the removal of organochlorine herbicide from spiked soils. *Science of The Total Environment*, 640, 629-636.
20. Ruiz, C., Mena, E., Cañizares, P., Villaseñor, J., & Rodrigo, M. A. (2013). Removal of 2, 4, 6-trichlorophenol from spiked clay soils by electrokinetic soil flushing assisted with granular activated carbon permeable reactive barrier. *Industrial & Engineering Chemistry Research*, 53(2), 840-846.
21. Santos, A., Fernández, J., Guadaño, J., Lorenzo, D., & Romero, A. (2018). Chlorinated organic compounds in liquid wastes (DNAPL) from lindane production dumped in landfills in Sabiñanigo (Spain). *Environmental Pollution*, 242, 1616-1624.
22. Souza, F. L., Sáez, C., Lanza, M. R. V., Cañizares, P., & Rodrigo, M. A. (2017). Removal of chlorsulfuron and 2, 4-D from spiked soil using reversible electrokinetic adsorption barriers. *Separation and Purification Technology*, 178, 147-153.

23. Souza, F. L., Saéz, C., Llanos, J., Lanza, M. R., Cañizares, P., & Rodrigo, M. A. (2016). Solar-powered electrokinetic remediation for the treatment of soil polluted with the herbicide 2, 4-D. *Electrochimica Acta*, 190, 371-377.
24. Sun, Y., Gao, K., Zhang, Y., & Zou, H. (2017). Remediation of persistent organic pollutant-contaminated soil using biosurfactant-enhanced electrokinetics coupled with a zero-valent iron/activated carbon permeable reactive barrier. *Environmental Science and Pollution Research*, 24(36), 28142-28151.
25. Jurado, E., Fernández-Serrano, M., Nunez-Olea, J., Luzon, G., & Lechuga, M. (2006). Simplified spectrophotometric method using methylene blue for determining anionic surfactants: applications to the study of primary biodegradation in aerobic screening tests. *Chemosphere*, 65(2), 278-285.

Figures

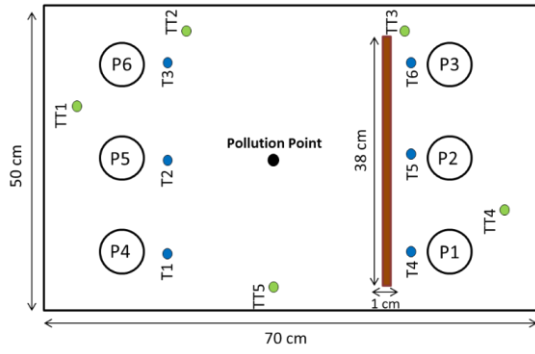


Figure SM1. Dimensions of the setup used. P1, 2 and 3: anodic wells; P4, 5 and 6: cathodic wells; T: tensiometers; TT: thermocouples.